Available online at www.sciencedirect.com
SCIENCE DIRECT
Journal of Power Sources 156 (2006) 315–320
JOURNAL OF POWER SOURCES
www.elsevier.com/locate/jpowsour

Combined activation methods for proton-exchange membrane fuel cells

Zhiqiang Xu [a], Zhigang Qi [b,*,1], Chunzhi He [c], Arthur Kaufman [d]

[a] *SKC PowerTech., 850 Clark Drive, Mt. Olive, NJ 07828, USA*
[b] *Plug Power Inc., 968 Albany Shaker Road, Latham, NY 12110, USA*
[c] *Columbian Chemicals Company, 1800 West Oak Commons Court, Marietta, GA 30062, USA*
[d] *69 Burnett Terrace, West Orange, NJ 07052, USA*

Received 29 March 2005; accepted 9 May 2005
Available online 25 July 2005

Abstract

Activating a PEM fuel cell by combining various activation methods could achieve a better performance than if only a single method was used. The combination of the following activation methods, (a) elevated temperature and pressure, (b) hydrogen evolution, and (c) CO oxidative stripping, was studied. First, any of these activation methods could largely increase the fuel cell performance more than a traditional break-in procedure. Second, the effectiveness of the individual methods was in the following sequence: (a) > (b) ≥ (c). Third, if method (a) was carried out after either method (b) or (c), the fuel cell performance could be further increased; but the final performance would be similar to that from just carrying out method (a) itself. Fourth, carrying out either method (b) or (c) after method (a) could further increase the fuel cell performance.

Keywords: Proton-exchange membrane fuel cell; Activation using elevated temperature and pressure; Hydrogen evolution; Hydrogen pumping; CO oxidative stripping; Incubation

1. Introduction

In order to reduce the cost of a proton-exchange membrane (PEM) fuel cell, catalysts supported on carbon particles have been widely used to make the electrodes. These supported catalysts have particle sizes of several nanometers and surface area of about 100 $m^2\,g^{-1}$ [1–3].

Another important component within the catalyst layer is a proton-conducting electrolyte, such as Nafion. In the anode where protons are produced via hydrogen oxidization, the proton-conducting electrolyte transports these protons through the anode catalyst layer to reach the membrane. In the cathode where protons are consumed with electrons and oxygen to form water, the proton-conducting electrolyte provides a pathway for transporting the protons from the membrane to the entire cathode catalyst layer. Hence, the presence of a proton-conducting electrolyte enables the catalyst layers to be active in three dimensions [4–10]. Otherwise, only the catalyst that is in a direct contact with the membrane will be active, and the majority of the remaining catalyst is wasted.

One beneficial feature of a PEM fuel cell is its low operating temperature. This low operating temperature assures its instant start-up, and thus makes a PEM fuel cell very suitable power sources for portable electronics and for backing-up telecommunication systems.

When a newly fabricated, low catalyst loading PEM fuel cell is operated under ambient conditions, it does not reach the best performance immediately. A so-called pre-conditioning or break-in period is needed. During this period, the cell performance normally increases gradually. Depending on the MEAs, a pre-conditioning could take many hours and even days. This not only consumes a lot of hydrogen fuel, but also slows down the entire fuel cell commissioning process.

We recently discovered that after the completion of a traditional break-in process the performance of a PEM fuel cell could be significantly increased further by carrying out

* Corresponding author. Tel.: +1 518 738 0229; fax: +1 518 782 7914.
E-mail address: zhigang_qi@plugpower.com (Z. Qi).
[1] This work was initially done at H Power Corporation.

0378-7753/$ – see front matter © 2005 Elsevier B.V. All rights reserved.
doi:10.1016/j.jpowsour.2005.05.072

certain novel activation procedures [11–16]. One activation procedure includes exposing the fuel cell to an elevated temperature and pressure [11–13]. After less than 2 h of running the cell under an aggressive condition, such as 75 °C of cell temperature, 95 °C of hydrogen humidification temperature, 90 °C of air humidification temperature, hydrogen back pressure of 20 psig, and air back pressure of 30 psig, the fuel cell performance could be boosted dramatically. For instance, the current density at certain cell voltages could be doubled after this activation procedure.

Another activation procedure involves hydrogen evolution at the electrode that is intended for activation [14,15]. Specifically, if we want to activate the cathode, hydrogen will be passed through the anode, and an external power source is applied to the fuel cell with the cathode side having a lower voltage than the anode side. Hydrogen at the anode is oxidized to form protons, and these protons are transported through the membrane to the cathode, where they are reduced to form hydrogen. When hydrogen evolves from the cathode electrode, it could change the porosity and tortuosity of the catalyst layer, leading to an increase in the number of reactant-catalyst-electrolyte three-phase sites. This increase in catalyst utilization therefore results in better fuel cell performance. Hydrogen evolution is often called hydrogen pumping as well because the final result is that hydrogen is moved from one side of the membrane to the other side of the membrane.

The third activation procedure is related to CO adsorption [16]. Since CO can strongly adsorb onto the catalyst surface, it poisons an electrode even at a concentration level of a few parts per million (ppm) [17–22]. Such poisoning has become a major obstacle to the development and commercialization of PEM fuel cells. The adsorbed CO can be removed by applying a positive potential to oxidize it to CO_2. We found that when CO_2 evolves from the catalyst surface, the electrode could also be activated [16].

This paper reports a new finding about the activation of PEM fuel cells. We found that by combining the aforementioned first method with either the second or third method, in a specified order, a PEM fuel cell could achieve performance better than if only a single method were used.

2. Experimental

2.1. Preparation of electrodes and MEAs

Catalyst mixtures were prepared by directly mixing supported catalysts with a Nafion solution (5%, DuPont) as described in [23]. The Nafion content within the mixture was controlled at 30%. The mixture was stirred thoroughly before it was applied onto a gas diffusion medium such as ELAT or carbon paper. The electrodes were dried in an oven at 135 °C for 30 min, and then were hot-bonded onto a Nafion 112 membrane at 130 °C for 3 min to form a membrane-electrode assembly (MEA).

When a commercial catalyst-coated membrane (CCM) was studied, a carbon paper-type gas diffusion medium was attached to both the anode and cathode catalyst layers without any bonding.

2.2. Testing of MEAs

Single cell tests were carried out using a homemade 10 cm^2 active area test fixture. The test fixture was composed of a pair of metal plates with single path serpentine flowfields. The plates were coated with metal nitride for corrosion protection. Rod-like heaters were inserted into the plates to control the cell temperature. During the fuel cell operation, the load was varied using a rheostat. Air and pure hydrogen were used as the reactants. They were passed through stainless steel water bottles prior to entering the cell to achieve a 100% relative humidity. The cell temperature, hydrogen humidification temperature, and air humidification temperature are denoted hereinafter as $T_{cell}/T_{H_2}/T_{air}$. Throughout this paper, both the hydrogen and air humidification temperatures refer to the bubblers' temperatures, which are higher than the reactant inlet dew point temperatures due to the heat loss through the tubing. The flow rates of air and hydrogen were controlled using flow meters to about 10 times stoichiometric for a current density of 2.0 A cm^{-2}. The polarization measurement was taken by controlling the cell voltage and recording the corresponding, stabilized current. The current normally stabilized quickly, and each point was taken in about 1 min.

2.3. Activation procedure by using elevated temperature (T) and pressure (P)

This elevated *T*/*P* activation was carried out at a cell temperature of 75 °C, hydrogen humidification temperature of 95 °C, air humidification temperature of 90 °C, hydrogen back pressure of 20 psig, and air back pressure of 30 psig. Such an activation condition is denoted hereinafter as 75/95/90 °C, 20/30 psig. During the activation, the fuel cell performance was recorded every 30 min. When no further increase in performance was observed, the activation procedure was considered to be complete.

2.4. Activation procedure by hydrogen evolution (or hydrogen pumping)

For this procedure, air at the cathode side was replaced by nitrogen, while the anode side was fed with pure hydrogen. An external power supply was used to generate a current density of ca. 200 mA cm^{-2} through the cell with hydrogen being oxidized at the anode, the protons transporting through the membrane to the cathode, and being reduced at the cathode. This procedure was carried at the cell temperature that was 35 °C, and lasted for 30 min. The reduction of protons resulted in hydrogen evolution at the cathode.

2.5. Activation procedure by CO oxidative stripping

It was performed at the cell temperature of 35 °C and consisted of two steps: an initial adsorption of CO onto the catalyst surface, followed by a potential sweeping to oxidize CO into CO_2. We call the whole process CO oxidative stripping. During the CO adsorption process, a mixed gas containing 0.5% CO (balanced by 99.5% nitrogen) was used at the cathode side, and the cathode voltage was set at 0.50 V. At such a potential, hydrogen evolution was not possible, and thus, the effect was solely due to CO oxidative stripping. The potential sweeping was carried out between 0.5 and 1.0 V at a scan rate of 30 mV s^{-1} in the presence of nitrogen. After CO is oxidized to CO_2, the latter should leave the catalyst surface readily because it has a very weak adsorption onto the catalyst surface.

During the CO oxidative stripping, the cyclic voltammograms of CO oxidation was recorded using a Solartron SI 1280B electrochemical measurement unit.

3. Results and discussion

In this study, since pure hydrogen was used as the fuel, the entire fuel cell performance was determined by the cathode. Therefore, the activation was focused on the cathode.

Fig. 1 shows effect of combining activation at elevated *T*/*P* with CO oxidative stripping on the performance of an MEA whose cathode consisted of 30% of Nafion and 70% of E-TEK 20% Pt/Vulcan XC-72 with a Pt loading of 0.17 mg cm^{-2}. The test was carried out at a cell temperature of 35 °C, hydrogen and air humidification temperature of 45 °C (35/45/45 °C). Curve 1 was the performance of the cell after over 4 h of break-in process. The break-in procedure was carried out by setting up the cell voltage at about 0.4 V for most of the time, and periodically sweeping the load from OCV to about 0.1 V at the above temperatures. During this process, the cell performance increased gradually, but after about 3 h, no apparent further increase was observed. At this point, we considered the break-in procedure to be complete.

Then three CO oxidative stripping cycles were carried out. The fuel cell performance after the first, second, and third CO oxidative stripping is represented by curves 2, 3, and 4, respectively. Unambiguously, sizable increase in the fuel cell performance was achieved after each CO oxidative stripping. When a fourth CO oxidative stripping was carried out, no further increase was observed (not shown). Therefore, curve 4 represents the best performance of this MEA that could be achieved by using CO oxidative stripping.

The fuel cell was then exposed to an elevated *T*/*P* procedure at 75/95/90 °C and 20/30 psig for 1 h. After the condition was returned to 35/45/45 °C, its performance was measured again. Curve 5 in Fig. 1 illustrates the result. Clearly, the fuel cell performance was further increased.

Actually, without carrying out the four cycles of CO oxidative stripping, the fuel cell could also achieve the performance shown by curve 5 by just carrying out the elevated *T*/*P* activation. In other words, if an activation using elevated *T*/*P* is carried out, there is no need to carry out any prior CO oxidative stripping activation from the performance point of view.

However, it was discovered that if a CO oxidative stripping was carried out after an activation using elevated *T*/*P*, the fuel cell performance could be further increased, as shown by curve 6 in Fig. 1. This performance could not be achieved if another activation using elevated *T*/*P* were repeated following the first one. Clearly, CO oxidative stripping could further enhance a fuel cell's performance when carried out after an elevated *T*/*P*.

Similar tests were carried out with a catalyst-coated membrane (CCM) whose cathode Pt loading was 0.3 mg cm^{-2}, and the results are shown in Fig. 2. Curve 7 was the fuel cell performance after the break-in procedure was complete. Curves 8 and 9 represent the performance after two cycles of CO oxidative stripping. When a third CO oxidative stripping was carried out, the performance was similar to curve 9.

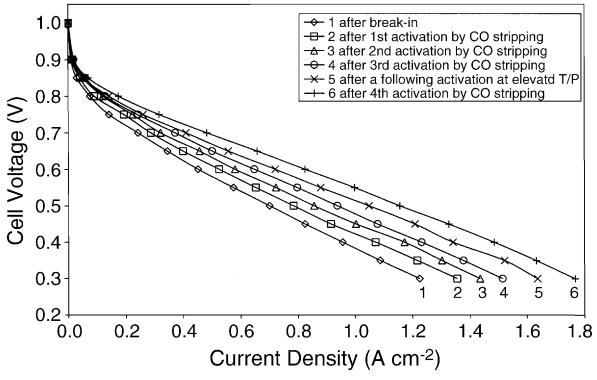

Fig. 1. Effect of combining CO oxidative stripping with elevated temperature and pressure on fuel cell performance. 35/45/45 °C; E-TEK 20% Pt/C; Pt loading 0.17 mg cm^{-2}; Nafion 112 membrane; ELAT gas diffusion medium.

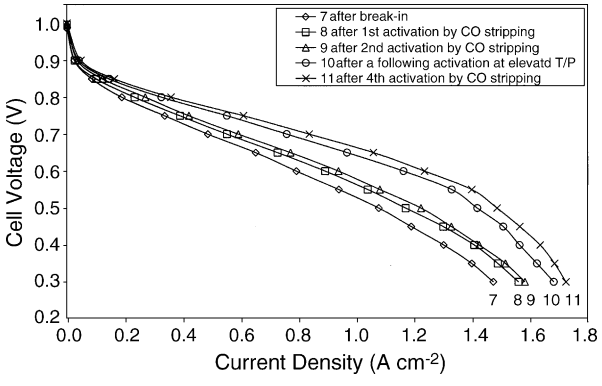

Fig. 2. Effect of combining CO oxidative stripping with elevated temperature and pressure on fuel cell performance. 35/45/45 °C; a commercial CCM with a Pt loading of 0.30 mg cm^{-2} and a 25 μm thickness membrane; Toray paper gas diffusion medium.

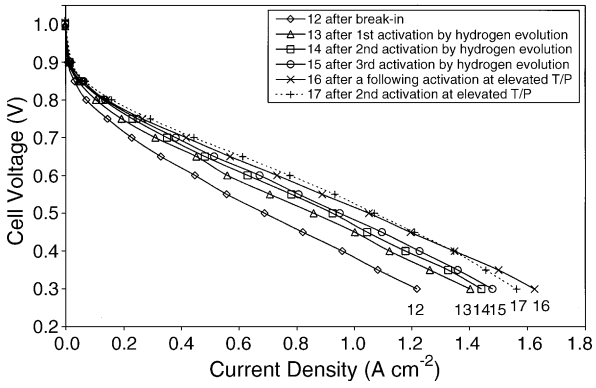

Fig. 3. Effect of combining hydrogen evolution with elevated temperature and pressure on fuel cell performance. 35/45/45 °C; E-TEK 20% Pt/C; Pt loading 0.17 mg cm^{-2}; Nafion 112 membrane; ELAT gas diffusion medium; 200 mA cm^{-2} hydrogen evolution current density and lasted for 30 min each time.

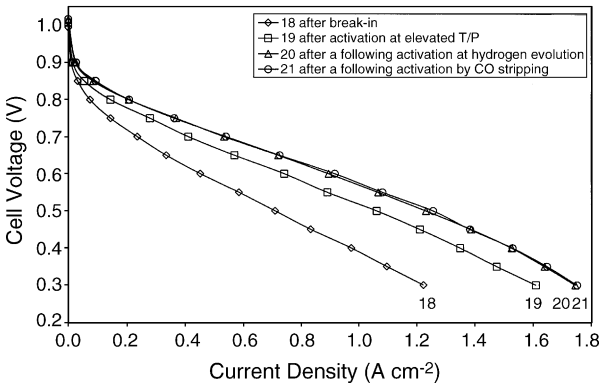

Fig. 4. Effect of combining elevated temperature and pressure with hydrogen evolution as well as CO oxidative stripping on fuel cell performance. 35/45/45 °C; E-TEK 20% Pt/C; Pt loading 0.17 mg cm^{-2}; Nafion 112 membrane; ELAT gas diffusion medium.

Hence, curve 9 represents the best performance that could be achieved by CO oxidative stripping. Then an activation using elevated *T*/*P* was carried out at 75/95/90 °C and 20/30 psig for 1 h. The fuel cell performance at 35/45/45 °C afterwards is shown as curve 10. Apparently, a dramatic increase was achieved by the elevated *T*/*P* activation. When an additional CO oxidative stripping was carried out, the fuel cell performance was boosted again, as shown by curve 11.

The effect of combing activation using elevated *T*/*P* with hydrogen evolution on fuel cell performance is shown in Fig. 3. Curve 12 was the performance after the completion of a traditional break-in procedure. Curves 13, 14, and 15 were the performance after three cycles of hydrogen evolution. The first hydrogen evolution increased the fuel cell performance more than the second, and the second was more than the third. Afterwards, the fuel cell was exposed to elevated *T*/*P* at 75/95/90 °C and 20/30 psig for 1 h. Following this activation, the fuel cell performance at 35/45/45 °C was tested again and the result is shown in Fig. 3 as curve 16. An additional increase in performance was achieved by this activation. When a second activation using elevated *T*/*P* was carried out, the fuel cell performance increased slightly at current densities less than ca. 1.3 A cm^{-2}, but it declined slightly at current densities higher than 1.3 A cm^{-2}.

Fig. 4 shows the combination effect when activation using elevated *T*/*P* was carried out before hydrogen evolution and CO oxidative stripping. Significant increase in performance was observed after the activation step using elevated *T*/*P* at 75/95/90 °C and 20/30 psig for 1 h shown by curve 19 (versus 18). Then a hydrogen evolution step was conducted, and a further performance increase was achieved (curve 20 versus 19). After the hydrogen evolution, a CO oxidative stripping was carried out, but no performance increase was observed (curve 21 versus 20). These results indicate that either a hydrogen evolution or a CO oxidative stripping alone following an activation using elevated *T*/*P* was able to push the fuel cell to the maximum performance.

Without mass transport limitation, fuel cell performance follows Eq. (1):

$$V = V_o – (b \log I) – RI \quad (1)$$

where V is the cell voltage in mV, V_o the cell voltage at minimal current densities, which can be taken as the open circuit voltage (mV), b the Tafel slope in mV decade^{-1}, R the total cell resistance in Ω cm^2, and I is the current density in mA cm^{-2}. Theoretically, b should be a negative number; but since a minus sign is used before the term [$b \log I$] in Eq. (1), a positive b value will be used in the following simulation.

In order to determine which factors in Eq. (1) were affected by activation procedures, experimental data were fitted using Eq. (1). During the fitting process, a very small current density of 0.00005 A cm^{-2} was arbitrarily assigned to open circuit voltage (OCV) to avoid log 0. Then all the data points were fitted according to Eq. (1) to get V_o, b and R. The symbols in Fig. 5 were experimental data obtained after an MEA was tested in the sequence of break-in, activation using elevated *T*/*P*, and activation using CO oxidative stripping. Clearly, both activation methods increased the fuel cell performance. The dotted lines in Fig. 5 were calculated according to Eq. (1)

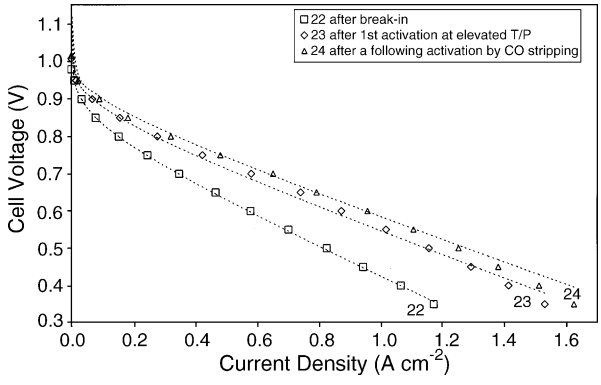

Fig. 5. Curve fitting to experimental data: symbols – data; dotted curves – fitting. 35/45/45 °C; E-TEK 20% Pt/C; Pt loading 0.25 mg cm^{-2}; Nafion 112 membrane; ELAT gas diffusion medium.

Table 1
Tafel slope and cell total resistance obtained from fitting experimental data

Methods	Break-in	Elevated *T*/*P*	CO stripping
b (mV decade^{-1})	85	72	65
R (Ω cm^2)	0.36	0.29	0.28
V_o (mV)	990	1003	1010
Measured OCV (mV)	930	960	967

using V_o, b and R obtained from fitting the data. Pretty good agreement was achieved for the data points at current densities less than 1.2 A cm^{-2} before mass transport resistance became serious. The values of b, R, and V_o obtained from the fitting are presented in Table 1. V_o is apparently larger than the measured OCV, and a major reason is that Eq. (1) does not take the reactant crossover current into consideration.

As indicated by Table 1, both the total cell resistance and Tafel slope decrease after the activation procedures are carried out. For the resistance, a large decrease was observed after the activation procedure using elevated *T*/*P*. This decrease in resistance is believed to be mainly related to the ionic resistance. The ionic resistance includes both the membrane resistance and the catalyst layer resistance. Based on the decline in resistance, it can be concluded that effective hydration of both the membrane and the ionomer within the catalyst layer is one of the accomplishments achieved by the activation using elevated *T*/*P*. Electrochemical impedance spectroscopy technique will be used to verify this in the future experiments. Based on the significant decline in the Tafel slope, it can be concluded that the catalyst layer structure is effectively changed to lead to an increased utilization or activity of the catalysts. Further activation using CO oxidative stripping did not further reduce the ionic resistance much, indicating that its activation mechanism is little related to ionomer hydration. The apparent decrease in Tafel slope and the increase in fuel cell performance are more likely related to the structural change of the catalyst layer. The structural change could be the porosity and tortuosity change of the catalyst layer, perhaps due to rearrangement or redistribution of the components within the catalyst layer.

The charge from CO oxidation is one of the parameters people use to estimate the total catalyst surface area within a catalyst layer. Since CO oxidation peak is very sharp and well defined, it is much easier to calculate the charge under this peak than that under hydrogen adsorption/desorption peaks. Fig. 6 shows the CO oxidation peaks after break-in, elevated *T*/*P*, and CO oxidative stripping, respectively, for the MEA shown in Fig. 5. The increase in peak height accompanying activations indicates that activations increased the catalyst utilization. However, the difference in peak height itself could not explain the large difference in performance. In particular, the peak became smaller after CO oxidative stripping, while the fuel cell performance was apparently increased. Obviously, the size of CO oxidation peak cannot be simply translated into fuel cell performance.

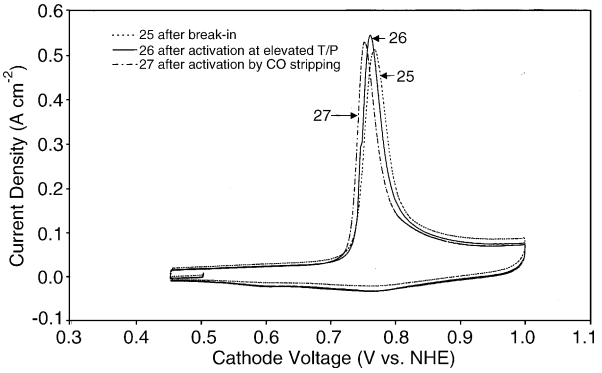

Fig. 6. Cyclic voltammograms of the first cycle during CO oxidation after the fuel cell break-in, activation using elevated temperature and pressure, and activation by CO stripping. 35/45/45 °C; E-TEK 20% Pt/C; Pt loading 0.25 mg cm^{-2}; Nafion 112 membrane; ELAT gas diffusion medium; potential scan rate 30 mV s^{-1}.

4. Conclusions

The activation or incubation of PEM fuel cells by a combination of three different activation methods was studied. These activation methods were (a) elevated temperature and pressure, (b) hydrogen evolution, and (c) CO oxidative stripping. Any one of these methods was effective to activate a PEM fuel cell, but the activation was not complete by using a single method alone. When method (b) or (c) was carried out before method (a), the activation result was similar to that achieved by method (a) itself. In other words, there is no need to carry out any activation according to method (b) or (c) before implementation of method (a). However, when method (b) or (c) was carried out after method (a), the fuel cell performance could be further improved, and in this case, using either method (b) or (c) achieved a similar result. Therefore, the best combination of activation procedures would be carrying out an activation using elevated temperature and pressure, then carrying out either hydrogen evolution or CO oxidative stripping.

Acknowledgements

The authors are grateful to Dr. John Elter, Mr. Daniel Beaty, and Ms. Cynthia Mahoney White of Plug Power for their review of this article and for their permission to publish the results.

References

[1] H.G. Petrow, R.J. Allen, US Patent 4,166,143 (1979).
[2] I.D. Raistrick, US Patent 4,876,115 (1989).
[3] H.G. Petrow, R.J. Allen, US Patent Re. 33,149 (1990).
[4] E.A. Ticianelli, C.R. Derouin, A. Redondo, S. Srinivasan, J. Electrochem. Soc. 135 (1988) 2209.
[5] Z. Poltarzewski, P. Staiti, V. Alderucci, W. Wieczorek, N. Giordano, J. Electrochem. Soc. 139 (1992) 761.

[6] M.S. Wilson, S. Gottesfeld, J. Electrochem. Soc. 139 (1992) L28.
[7] M.S. Wilson, S. Gottesfeld, J. Appl. Electrochem. 22 (1992) 1.
[8] M.S. Wilson, US Patent 5,211,984 (1993).
[9] Y. Fukuoka, M. Uchida, N. Eda, US Patent 5,723,173 (1998).
[10] M. Watanabe, K. Sakairi, US Patent 5,728,485 (1998).
[11] Z. Qi, A. Kaufman, J. Power Sources 111 (2002) 181.
[12] Z. Qi, A. Kaufman, J. Power Sources 114 (2003) 21.
[13] Z. Qi, A. Kaufman, US Patent 6,805,983 (2004).
[14] C. He, Z. Qi, M. Hollett, A. Kaufman, Electrochem. Solid-State Lett. 5 (2002) A181.
[15] C. He, Z. Qi, A. Kaufman, US Patent 6,730,424 (2004).
[16] Z. Xu, Z. Qi, A. Kaufman, J. Power Sources. 156 (2006) 281.
[17] V.M. Schmidt, H.-F. Oetjen, J. Divisek, J. Electrochem. Soc. 144 (1997) 237.
[18] R.J. Bellows, E. Marucchi-Soons, R.P. Reynolds, Electrochem. Solid-State Lett. 1 (1998) 69.
[19] S.J. Lee, S. Mukerjee, E.A. Ticianelli, J. McBreen, Electrochim. Acta 44 (1999) 3283.
[20] S. Mukerjee, S.J. Lee, E.A. Ticianelli, J. McBreen, B.N. Grgur, N.M. Markovic, P.N. Ross, J.R. Giallombardo, E.S. De Castro, Electrochem. Solid-State Lett. 2 (1999) 12.
[21] B.N. Grgur, N.M. Markovic, P.N. Ross, J. Electrochem. Soc. 146 (1999) 1613.
[22] K.Y. Chen, Z. Sun, A.C.C. Tseung, Electrochem. Solid-State Lett. 3 (2000) 10.
[23] Z. Qi, A. Kaufman, J. Power Sources 113 (2003) 37.